

Cover Page



Universiteit Leiden



The handle <http://hdl.handle.net/1887/80327> holds various files of this Leiden University dissertation.


Author: Dvornik, A.

Title: The galaxy–dark matter connection: a KiDS study

Issue Date: 2019-11-13

5

KiDS+GAMA: Inferring satellite halo masses using two-dimensional shear maps

 E use data from the Kilo-Degree Survey (KiDS) and the Galaxy And Mass Assembly (GAMA) surveys to simultaneously constrain the stellar-to-halo mass relations of both central and satellite galaxies of spectroscopically confirmed galaxies in galaxy groups using weak lensing. For the analysis we use the traditional one-dimensional method in the form of the stacked tangential shear measurements to determine the halo and subhalo masses of our galaxies and to constrain the stellar-to-halo mass relation, as well as a two-dimensional fit to the full shear field that uses all the available information about lens galaxies and exact source galaxies positions and ellipticities. We find that the two-dimensional method performs better than the one-dimensional method statistically by a factor of ~ 2 . Both methods lead to similar parameters of the stellar-to-halo mass relation, which are consistent with previous results found in the literature, showing that the satellite galaxies have generally lower halo masses than the central galaxies, given the same stellar mass.

A. Dvornik, K. Kuijken, H. Hoekstra, with KiDS and GAMA collaborations

5.1 INTRODUCTION

According to the hierarchical galaxy formation model, galaxy groups and clusters form by accretion of isolated galaxies and groups. Such an assembly process will tidally strip mass from the infalling satellite galaxies/haloes. Because the dark matter is dissipationless it will be more easily stripped from the subhalo than the baryons, which will dissipate some of their energy and sink to the centre of their potential well before forming stars (White & Rees 1978). This model thus predicts that the satellite galaxies will be preferentially stripped of their dark matter and the effect can be observed as higher stellar mass to halo mass ratios of satellite galaxies compared to their central counterparts of similar stellar mass.

While the stellar-to-halo mass relation of central galaxies has been successfully measured by many studies (for instance by Hoekstra et al. 2005; Mandelbaum et al. 2006; More et al. 2011; van Uitert et al. 2011; Leauthaud et al. 2012), this is not the case for satellite galaxies whose stellar-to-halo mass relation remains essentially unconstrained (Sifón et al. 2018). Recently, several weak gravitational lensing studies using galaxy groups and clusters have been undertaken (such as the ones by Limousin et al. 2007; Li et al. 2014b, 2016; Sifón et al. 2015, 2018), all finding that the satellite galaxies are heavily truncated with the respect to the central and field galaxies. All the previous simulation studies (Bower et al. 2006) show that the stellar-to-halo mass relation of satellite galaxies is significantly different from the stellar-to-halo mass relation of central galaxies.

In order to measure the stellar-to-halo mass ratio of satellite galaxies, one needs to estimate the total mass of satellite galaxies. Weak gravitational lensing, through the lensing of background sources by a sample of galaxies – commonly called galaxy-galaxy lensing, directly measures the total mass of lensing galaxies, without assuming their dynamical state (Bartelmann & Schneider 2001; Courteau et al. 2014), and it is currently the only method available to measure the total mass of samples of galaxies directly. Measuring the lensing signal around satellite galaxies, however, can be particularly challenging for several reasons: a small contribution to the lensing signal by the host galaxy group, source blending at small separations and sensitivity to field galaxy contamination (Sifón et al. 2018). As pointed out by Sifón et al. (2015), the latter point is quite important as the field galaxies will not be stripped and the contamination complicates the interpretation of the lensing signal.

To overcome the aforementioned challenges in measuring the satellite galaxies' lensing signal in this study we use the two-dimensional galaxy-galaxy lensing method, first proposed by Schneider & Rix (1997), to analyse galaxy-galaxy lensing data. The two-dimensional galaxy-galaxy lensing method tries to fit a two-dimensional shear field directly to the galaxy ellipticity measurements, and it was shown to perform significantly better for dense lens populations, compared to the traditional one-dimensional method in the form of the stacked tangential shear estimates or excess surface density (ESD) profiles (**Chapter 4**).

This method went out of fashion due to the unavailability of galaxy grouping information that would accurately classify galaxies as centrals and satellites (Hoekstra 2014), the same information needed to robustly study the stellar mass to halo mass

relation of satellite galaxies (Sifón et al. 2015). Treating the galaxies as centrals and satellites in a statistical way when considering the stacked signal could be naturally accounted for with the halo model (Seljak 2000; Peacock & Smith 2000; Cooray & Sheth 2002), thus overcoming the observational shortcomings. In recent years the galaxy grouping information has become available thanks to the power of wide-field photometric surveys (for instance KiDS; Kuijken et al. 2015; de Jong et al. 2015) complemented with spectroscopic group information (from spectroscopic surveys like Galaxy And Mass Assembly (hereafter GAMA) survey; Driver et al. 2011; Robotham et al. 2011) that allow one to treat the central and satellite galaxies deterministically. One important advantage of the two-dimensional method lies in the fact that it exploits all the information of the actual image configuration (the model predicts the shear for each individual background galaxy image) using the galaxies' exact positions, ellipticities, magnitudes, luminosities, stellar masses, group membership, information, etc., rather than using only the ensemble properties of statistically equivalent samples (Schneider & Rix 1997). Moreover, the clustering of the lenses is naturally taken into account, although it is more difficult to account for the expected diversity in density profiles (Hoekstra 2014).

In this paper we present a two-dimensional galaxy-galaxy lensing measurement of the stellar-to-halo mass relation for central and satellite galaxies, by combining a sample of spectroscopically confirmed galaxy groups from the Galaxy And Mass Assembly survey (Driver et al. 2011) and background galaxies from the Kilo-Degree Survey (**Chapter 6**). We use these measurements to constrain the stellar-to-halo mass relation using both one-dimensional stacked tangential shear profiles and the two-dimensional galaxy-galaxy lensing method.

The outline of this paper is as follows. In Sec. 5.2 we present the lens and source sample used in this analysis. In Sec. 5.3 we present the two-dimensional galaxy-galaxy lensing formalism and in Sec. 5.4 we present the specific lens model used in the paper. We present the results in Sec. 5.5 and conclude with Sec. 5.6. Throughout the paper we use the following cosmological parameters entering in the calculation of the distances and other relevant properties (Planck Collaboration et al. 2013): $\Omega_m = 0.307$, $\Omega_\Lambda = 0.693$, $\sigma_8 = 0.8288$, $n_s = 0.9611$, $\Omega_b = 0.04825$ and $h = 0.6777$. The halo masses are defined as $M = 4\pi r_\Delta^3 \Delta \bar{\rho}_m / 3$ enclosed by the radius r_Δ within which the mean density of the halo is Δ times the mean density of the Universe $\bar{\rho}_m$, with $\Delta = 200$. All the measurements presented in the paper are in comoving units.

5.2 DATA AND SAMPLE SELECTION

The foreground galaxies used in this lensing analysis are taken from the GAMA survey (Driver et al. 2011), a spectroscopic survey carried out on the Anglo-Australian Telescope with the AAOmega spectrograph. Specifically, we use the information of GAMA galaxies from three equatorial regions, G9, G12 and G15 from GAMA II (Liske et al. 2015). We do not use the G02 and G23 regions, because the first one does not overlap with KiDS and the second one uses a different target selection compared to the one used in the equatorial regions. These equatorial regions encom-

pass $\sim 180 \text{ deg}^2$, contain 180 960 galaxies (with $nQ \geq 3$, where the nQ is a measure of redshift quality) and are highly complete down to a Petrosian r -band magnitude $r = 19.8$. For this thesis Chapter we only use galaxies in the G9 field (a full KiDS and GAMA overlap study will be performed later on) and we use only the galaxies that reside in groups identified by Robotham et al. (2011). Inclusion of only the group galaxies might potentially bias our results, but we defer this analysis to the upcoming and complete study on the full GAMA area. The GAMA galaxy group catalogue was constructed using a 3-dimensional Friends-of-Friends (FoF) algorithm, linking galaxies in projected and line-of-sight separation. We use version 10 of the group catalogue (G3Cv10), which contains 26 194 (7481 in G9) groups with at least 2 members. Following (Viola et al. 2015), we restrict ourselves to galaxy groups with at least 5 members as low multiplicity groups are contaminated with interlopers (Robotham et al. 2011) and consider all the galaxies within those groups whose stellar mass is between $10^8 M_\odot$ and $10^{12} M_\odot$. Stellar masses are taken from version 20 of the LAMBDA stellar mass catalogue, described in Wright et al. (2017). The final selection of galaxies can be seen in Fig. 5.1 and Fig. 5.2, and all the relevant properties we need in our analysis are presented in Table 5.1. The stellar mass binning is used only for the one-dimensional galaxy-galaxy lensing case in order to obtain stacks of tangential shear signal. In the two-dimensional case, we directly use the relevant galaxy quantities in the model.

We use imaging data from the 60 deg^2 of KiDS (**Chapter 6**) that overlaps with the G9 patch of the GAMA survey (Driver et al. 2011) to obtain shape measurements of background galaxies. KiDS is a four-band imaging survey conducted with the OmegaCAM CCD mosaic camera mounted at the Cassegrain focus of the VLT Survey Telescope (VST); the camera and telescope combination provide us with a fairly uniform point spread function across the field-of-view.

We use shape measurements based on the r -band images, which have an average seeing of 0.66 arcsec. The image reduction, photometric redshift calibration and shape measurement analysis is described in detail in Hildebrandt et al. (2018) and in **Chapter 6**. We measure galaxy shapes using *lensfit* (Miller et al. 2013), which has been calibrated using image simulations described in Kannawadi et al. (2019). This provides galaxy ellipticities (ϵ_1, ϵ_2) with respect to an equatorial coordinate system.

5.3 2D GALAXY-GALAXY LENSING FORMALISM

In this study of satellite galaxy-galaxy lensing we use the two-dimensional galaxy-galaxy lensing formalism as discussed in **Chapter 4**, following the model therein and adapting it to work with KiDS+GAMA data, taking into account the survey specific requirements. Generally, for both the one-dimensional and two-dimensional cases, the likelihood of a model with a set of parameters θ given data \mathbf{d} can be parametrised in the following form:

$$\mathcal{L}(\theta | \mathbf{d}) = \frac{1}{\sqrt{(2\pi)^n |\mathbf{C}|}} \exp \left[-\frac{1}{2} (\mathbf{m}(\theta) - \mathbf{d})^T \mathbf{C}^{-1} (\mathbf{m}(\theta) - \mathbf{d}) \right], \quad (5.1)$$

Table 5.1: Overview of the number of galaxies/lenses, median stellar masses of galaxies and median redshifts in each selected bin used for our one-dimensional stacked tangential shear analysis. Stellar masses are given in units of $[\log(M_\star/[M_\odot])]$.

Bin	Range	N_{tot}	N_{cen}	N_{sat}	$M_{\star,\text{med}}$	z_{med}
1	(8.0,10.0]	1004	3	1001	9.66	0.095
2	(10.0,10.2]	491	5	486	10.11	0.167
3	(10.2,10.4]	740	10	730	10.32	0.192
4	(10.4,10.6]	1034	29	1005	10.51	0.202
5	(10.6,10.8]	1295	53	1242	10.71	0.247
6	(10.8,11.0]	1298	108	1190	10.90	0.272
7	(11.0,11.2]	1016	235	781	11.09	0.282
8	(11.2,11.4]	513	229	284	11.28	0.282
9	(11.4,11.6]	239	171	68	11.47	0.294
10	(11.6,11.8]	40	36	4	11.66	0.314
11	(11.8,12.0]	5	3	2	11.88	0.271

where $\mathbf{m}(\theta)$ is the value of \mathbf{d} predicted by the model with parameters θ . We assume the measured data points $\mathbf{d} = [d_1, \dots, d_n]$ are drawn from a normal distribution with a mean equal to the true values of the data. The likelihood function accounts for correlated data points through the covariance matrix \mathbf{C} . The covariance matrix \mathbf{C} consists of two parts, the first one arising from shape noise and the second part from the presence of cosmic structure between the observer and the source (Hoekstra 2003):

$$\mathbf{C} = \mathbf{C}^{\text{shape}} + \mathbf{C}^{\text{LSS}}. \quad (5.2)$$

In the case when one wants to fit one-dimensional tangential shear profiles, stacked over a sample of lenses, the likelihood function can be written as:

$$\begin{aligned} \mathcal{L}(M_h, M_\star, c | \gamma_t^{\text{obs}}) & \quad (5.3) \\ &= \prod_i \frac{1}{\sigma_{g_{t,i}} \sqrt{2\pi}} \exp \left[-\frac{1}{2} \left(\frac{g_{t,i}(M_h, R, z) - g_{t,i}^{\text{obs}}}{\sigma_{g_{t,i}}} \right)^2 \right], \end{aligned}$$

where we have used $m_i = g_{t,i}(M_h, R, z)$ as the model prediction given halo mass M_h , radial bin R and redshift of the lens z , and the $d_i = g_{t,i}^{\text{obs}}$ as the tangentially averaged shear of a sample of lenses measured from observations. Here we have also used the uncertainty of our measurement, given by the $\sigma_{g_{t,i}}$ calculated from the intrinsic shape noise of sources in each radial bin. Moreover we assume that the variance σ^2 is the diagonal of the full covariance matrix:

$$\sigma = \sqrt{|\mathbf{C}|}, \quad (5.4)$$

i.e., we only account for the error due to the shape noise. Similarly, the likelihood function can be defined for the case when one would like to fit the two-dimensional

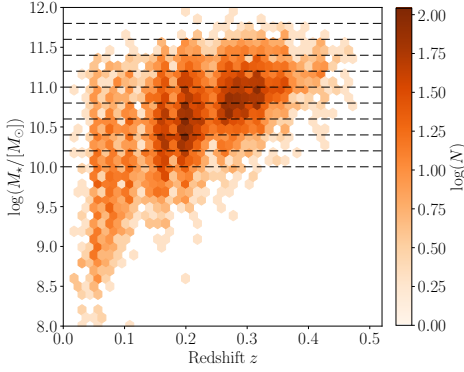


Figure 5.1: Stellar mass versus redshift of galaxies in rich groups in the G9 region of the GAMA survey that overlap with KiDS. The full sample is shown with hexagonal density plot and the dashed lines show the cuts for the stellar mass bins used in our analysis.

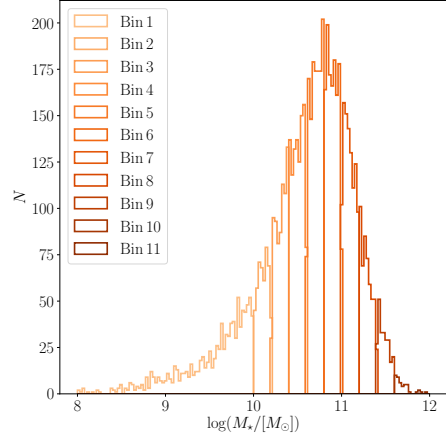


Figure 5.2: Stellar mass distributions in our 11 bins used for one-dimensional stacked tangential shear measurements. The exact bin values are presented in Table 5.1.

shear field:

$$\begin{aligned} \mathcal{L}(M_h, M_*, c | \epsilon^{\text{obs}}) & \quad (5.5) \\ &= \prod_i \frac{1}{\sigma_{\epsilon,i} \sqrt{2\pi}} \exp \left[-\frac{1}{2} \left(\frac{g_i(M_h, x_i, z) - \epsilon_i^{\text{obs}}}{\sigma_{\epsilon,i}} \right)^2 \right], \end{aligned}$$

where $g_i(M_h, x_i, z)$ are the reduced shears evaluated at each source position x_i , ϵ_i^{obs} the observed ellipticities of real galaxies and $\sigma_{\epsilon,i}$ is the intrinsic shape noise of our galaxy sample per component, calculated from the *lensfit* weights following the description by (Heymans et al. 2012) and it is the same as the $\sigma_{g_i,i}$. The same *lensfit* weights are used to weight the ϵ_i^{obs} as well. In practice, the two-dimensional fit to the ellipticities is carried out for each cartesian component of ellipticity ϵ_1 and ϵ_2 with respect to the equatorial coordinate system.

5.4 LENS MODEL

The most widely assumed density profile for dark matter haloes is the Navarro–Frenk–White (NFW) profile (Navarro et al. 1996). Using simple scaling relations this profile can be matched to simulated dark matter haloes over a wide range of masses and was found to be consistent with observations (Navarro et al. 1996). It is defined

as:

$$\rho_{\text{NFW}}(r) = \frac{\delta_c \bar{\rho}_m}{(r/r_s)(1+r/r_s)^2}, \quad (5.6)$$

where the free parameters δ_c and r_s are called the overdensity and the scale radius, respectively, and $\bar{\rho}_m$ is the mean density of the universe, where $\bar{\rho}_m = \Omega_m \rho_c$ and ρ_c is the critical density of the universe, defined by

$$\rho_c \equiv \frac{3H_0^2}{8\pi G}, \quad (5.7)$$

where H_0 is the present day Hubble parameter.

The NFW profile in its usual parametrisation has two free parameters for each halo, halo mass M_h and concentration c , and using those is the conventional way of modelling halo profiles. However, having two free parameters for each halo is computationally very expensive and not supported by the data. Rather we would like to describe these parameters through relations that depend on halo properties, and then fit to a few free parameters in these global relations instead of hundreds or thousands of free, halo-specific parameters. To do so, we adopt the halo mass – concentration relation of Duffy et al. (2008), with a free concentration normalisation f_c :

$$c(M_h, z) = f_c 10.14 \left[\frac{M_h}{(2 \times 10^{12} M_\odot / h)} \right]^{-0.081} (1+z)^{-1.01}, \quad (5.8)$$

We also adopt the stellar mass to halo mass relation in a shape of a single power law:

$$M_h = M_0 \left(\frac{M_\star}{10^{11} M_\odot} \right)^\alpha, \quad (5.9)$$

where α and M_0 are the free parameters we will be fitting. We use separate relations for the central and satellite galaxies, as we want to constrain the stellar-to-halo mass relation for those populations separately.

The gravitational shear and convergence profiles are then calculated using the equations presented by Wright & Brainerd (2000), from which the predicted ellipticities for all the lenses are calculated according to the weak lensing relations presented in Schneider (2003). We first calculate the reduced shear for our NFW profiles:

$$g(x_i, z_s) = \frac{\gamma(x_i, z_s)}{1 - \kappa(x_i, z_s)}, \quad (5.10)$$

from which the ellipticities are calculated according to the following equation:

$$\epsilon = \begin{cases} g & |g| \leq 1 \\ 1/g^* & |g| > 1 \end{cases}, \quad (5.11)$$

where we have assumed that the intrinsic ellipticities of the sources average to 0, due to their random nature.

We compute the effective critical surface mass density that we need in our lens model for each lens using the spectroscopic redshift of the lens z_1 and the full normalised redshift probability density of the sources, $n(z_s)$, calculated using the direct calibration method presented in Hildebrandt et al. (2017, 2018).

The effective inverse critical surface density can be written as:

$$\Sigma_{\text{cr,ls}}^{-1} = \frac{4\pi G}{c^2} (1 + z_1)^2 D(z_1) \int_{z_1}^{\infty} \frac{D(z_1, z_s)}{D(z_s)} n(z_s) dz_s, \quad (5.12)$$

where $D(z_1)$ is the angular diameter distance to the lens, $D(z_1, z_s)$ is the angular diameter distance between the lens and the source and $D(z_s)$ is the angular diameter distance to the source.

The galaxy source sample is specific to each lens redshift with a minimum photometric redshift $z_s = z_1 + \delta_z$, with $\delta_z = 0.2$, where δ_z is an offset to mitigate the effects of contamination from the group galaxies (for details see also the methods section and Appendix of **Chapter 2**). We determine the source redshift distribution $n(z_s)$ for each sample, by applying the sample photometric redshift selection to a spectroscopic catalogue that has been weighted to reproduce the correct galaxy colour-distributions in KiDS (for details see Hildebrandt et al. 2018). We correct the measured ellipticities for the multiplicative shear bias per source galaxy per redshift bin as defined in Hildebrandt et al. (2018) with correction values estimated from the image simulations (Kannawadi et al. 2019).

5.5 RESULTS

The free parameters for our model are listed in Table 5.2, together with their prior ranges. We use a Bayesian inference method in order to obtain full posterior probabilities using a Monte Carlo Markov Chain (MCMC) technique; more specifically we use the `emcee` Python package (Foreman-Mackey et al. 2013). The likelihoods we use are the same as given by Equations 5.3 and 5.5. We use wide flat priors for all the parameters (given in Table 5.2), which are the same for both our methods as well.

We run the sampler using 32 walkers, each with 50 000 steps (for a combined number of 1 600 000 samples), out of which we discard the first 5000 burn-in steps, 160 000 samples). The resulting MCMC chains are well converged according to the integrated autocorrelation time test.

We fit the lens model as described in Sect 5.4 to the measured stacked tangential shear measurements in our 11 stellar mass bins. A single stacked tangential shear profile for the GAMA lenses (blue points) in the $10^{11.2}$ to $10^{11.4} M_{\odot}$ stellar mass bin is shown in Fig. 5.3, with the measurements and their respective 1σ errors (orange lines and bands). The measured lens model best-fit parameters, together with their 68% credibility intervals are presented in Table 5.2. Their full posterior distributions are shown in Fig. 5.6. The resulting fit has a reduced $\chi^2_{\text{red}} (\equiv \chi^2/\text{d.o.f.})$ equal to 0.94, which is an appropriate fit, given the 93 degrees of freedom (d.o.f.).

The main results of this work are the stellar-to-halo mass relations for centrals and satellites, which for the one-dimensional study, we show in Fig. 5.4. The stellar-

Table 5.2: Priors and marginalised posterior estimates of the free parameters used in our lens model, for both the one-dimensional method and the two-dimensional method. All priors are uniform in linear space in the quoted range. The central values are calculated as median of the MCMC samples and the uncertainties are the 68% credibility interval.

	$\log(M_{0,\text{cen}}/M_{\odot})$	α_{cen}	$f_{c,\text{cen}}$	$\log(M_{0,\text{sat}}/M_{\odot})$	α_{sat}	$f_{c,\text{sat}}$
Priors	[5, 15]	[0, 5]	[0, 5]	[5, 15]	[0, 5]	[0, 5]
1D	$13.37^{+0.19}_{-0.25}$	$0.61^{+0.48}_{-0.40}$	$0.43^{+0.15}_{-0.12}$	$12.89^{+0.11}_{-0.13}$	$0.35^{+0.15}_{-0.15}$	$0.03^{+0.02}_{-0.01}$
2D	$13.44^{+0.11}_{-0.22}$	$0.85^{+0.09}_{-0.25}$	$0.49^{+0.17}_{-0.20}$	$12.91^{+0.05}_{-0.08}$	$0.47^{+0.14}_{-0.05}$	$0.09^{+0.03}_{-0.06}$

to-halo mass relations are completely described with two parameters each (two for centrals and two for satellites) – the normalisation M_0 and slope α , for which the obtained values for centrals and satellite are $\log(M_{0,\text{cen}}/M_{\odot}) = 13.37^{+0.19}_{-0.25}$, $\alpha_{\text{cen}} = 0.61^{+0.48}_{-0.40}$ and $\log(M_{0,\text{sat}}/M_{\odot}) = 12.89^{+0.11}_{-0.13}$, $\alpha_{\text{sat}} = 0.35^{+0.15}_{-0.15}$ respectively. As expected, the stellar-to-halo mass relations are significantly different for the central and satellite galaxies, showing that the stripping of the dark matter does indeed take place (the stellar-to-halo mass relation of satellite galaxies is lower than the one of the centrals). What is more, the width of the obtained stellar-to-halo mass relation is similar to the one that can be seen in simulations, for instance by the EAGLE hydrodynamical simulation (Schaye et al. 2015; Matthee et al. 2017).

The normalisations of the concentration-halo mass relation f_c are $f_{c,\text{cen}} = 0.43^{+0.15}_{-0.12}$ and $f_{c,\text{sat}} = 0.03^{+0.02}_{-0.01}$ for centrals and satellites, respectively, comparable to the values that are found in hydrodynamical simulations (**Chapter 4**). The concentration-halo mass normalisation is not significantly correlated with any of the other parameters of the stellar-to-halo mass relation, thus not significantly influencing our results. Those values are also consistent with the observational findings that prefer lower normalisations than expected in simulations, such as in the studies of Viola et al. (2015); Sifón et al. (2015); Dvornik et al. (2017).

For the two-dimensional results we can only present the obtained posterior distributions of our free parameters, as there is no direct representation of the results as in the case of one-dimensional galaxy-galaxy lensing. The measured lens model best-fit parameters, together with their 68% credibility intervals are presented in Table 5.2. Their full posterior distributions are shown in Fig 5.6. The resulting fit has a reduced χ^2_{red} ($\equiv \chi^2/\text{d.o.f.}$) equal to 0.92, with 2 235 297 degrees of freedom (d.o.f.), which means that the model is slightly over-fitting the data and a reduced set of parameters might be needed.

For the two-dimensional study we present the obtained stellar-to-halo mass relations in Fig. 5.5. The obtained values for centrals and satellite in the case when using the two-dimensional galaxy-galaxy lensing are $\log(M_{0,\text{cen}}/M_{\odot}) = 13.44^{+0.11}_{-0.22}$, $\alpha_{\text{cen}} = 0.85^{+0.09}_{-0.25}$ and $\log(M_{0,\text{sat}}/M_{\odot}) = 12.91^{+0.05}_{-0.08}$, $\alpha_{\text{sat}} = 0.47^{+0.14}_{-0.05}$ respectively, reported as well in Table 5.2. These results are comparable to the ones from the one-dimensional method and show that the two-dimensional method performs better statistically. Furthermore, we have not used all the galaxies in the G9 GAMA patch, leaving out the

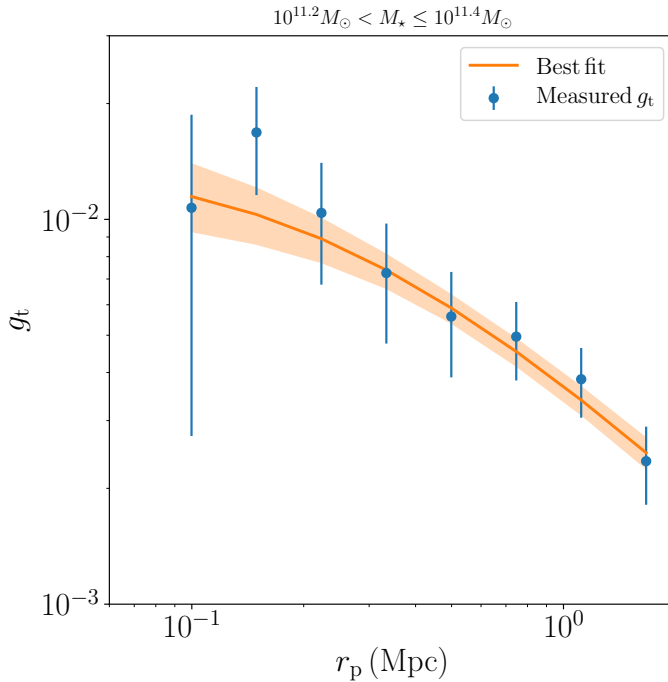


Figure 5.3: Stacked tangential shear profile for the GAMA lenses (blue points) in the $10^{11.2}$ to $10^{11.4}M_{\odot}$ stellar mass bin. The full orange line together with the orange band shows the best fitting lensing model for the 1D method, consisting of contribution from centrals and satellites and the 68% credibility interval, respectively.

groups with small member populations and all the isolated galaxies, thus possibly biasing our two-dimensional inference. Any galaxies left out of the analysis will bias the results up to 20% estimated for the KiDS and GAMA study (**Chapter 4**), mostly affecting the normalisation of the stellar-to-halo mass relation. To properly account for this, we need to repeat the analysis using all the available lens galaxies as well as test for the robustness of the central and satellite galaxy classification in the GAMA catalogue. The group catalogue is known to be contaminated by the misidentification of the central galaxy in a group, such that the true central galaxy would be included in the satellite sample, which can introduce roughly a 15% bias on the inferred masses (Sifón et al. 2015). What is more, the satellite stellar-to-halo mass relation at high stellar mass is possibly driven by the misidentification of satellite galaxies, which should actually be classified as centrals, given the high halo masses measured. This is a likely consequence of the observed problem with the Friends-of-Friend (FoF) algorithm used to identify galaxy groups in the GAMA survey, but it does not seem to largely affect the obtained results. The FoF algorithm will separate groups into

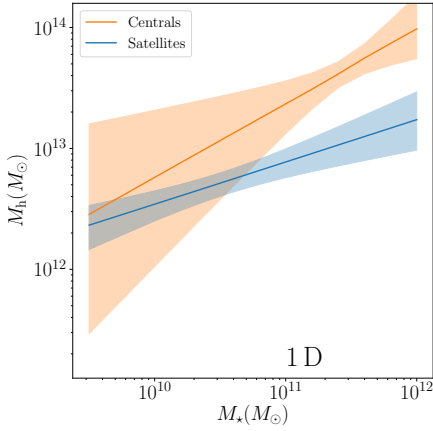


Figure 5.4: Stellar-to-halo mass relation for the central galaxies (orange) and satellite galaxies (blue) for the one-dimensional tangential shear analysis of GAMA groups. The solid lines show the median relation obtained from our MCMC fit and the orange and blue band show the 68% credibility interval for the inferred relation.

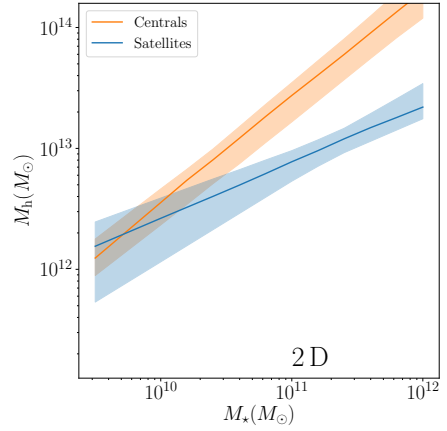


Figure 5.5: Stellar-to-halo mass relation for the central galaxies (orange) and satellite galaxies (blue) for the two-dimensional tangential shear analysis of GAMA groups. The solid lines show the median relation obtained from our MCMC fit and the orange and blue band show the 68% credibility interval for the inferred relation.

a number of smaller groups or aggregate smaller, unrelated groups into one large group, which would then host more than one central galaxy with them being classified as a satellite (Jakobs et al. 2018).

The normalisations of the concentration-halo mass relation $f_{c,\text{cen}}$ and $f_{c,\text{sat}}$ for centrals and satellites respectively, are also comparable to the ones for the one-dimensional method. They are less consistent with previous lensing measurements of GAMA galaxies (Viola et al. 2015; Sifón et al. 2015), especially for satellite galaxies, a fact that needs to be addressed in the future. The likely inconsistency might arise from the fact that Sifón et al. (2015) fixed the normalisation of the concentration-halo mass relation of satellite galaxies to 1. This might as well explain our over-fitting problem. The results show our ability to use the two-dimensional galaxy-galaxy lensing to constrain the stellar-to-halo mass relation of both central and satellite galaxies. The statistical performance of the two-dimensional method is better, as expected, but it is clearly noticeable that it might be significantly biased compared to the one-dimensional method.

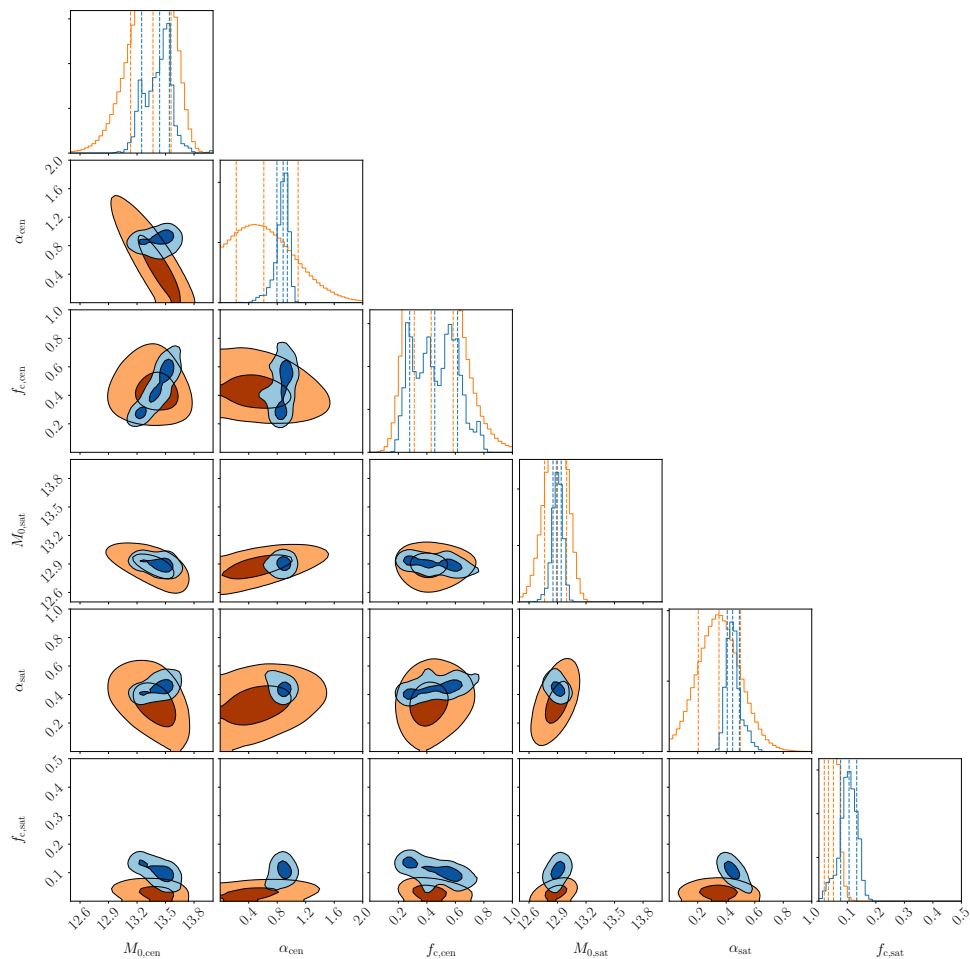


Figure 5.6: Full posterior distributions of the model parameters $M_{0,\text{cen}}$, α_{cen} , $f_{\text{c,cen}}$, $M_{0,\text{sat}}$, α_{sat} and $f_{\text{c,sat}}$, for both the one-dimensional stacked tangential shear measurements (in orange) as well as the two-dimensional galaxy-galaxy lensing method (in blue). The contours indicate the 1σ and 2σ credibility regions. Priors used in the MCMC fit can be seen in Table 5.2.

5.6 DISCUSSION AND CONCLUSIONS

We have made a preliminary measurement of the stellar-to-halo mass relation of central and satellite galaxies located in the GAMA groups. In this analysis we use the two-dimensional galaxy-galaxy lensing method to better constrain the stellar-to-halo mass relation, given the observed advantage of it over traditionally used stacked tangential shear method (also referred here as the one-dimensional galaxy-galaxy lensing, **Chapter 4**).

We use one of the equatorial GAMA patches (G9) that overlaps with the KiDS data in order to calculate both the tangential shear signal around the galaxies in rich groups with more than 5 members, and the two-dimensional galaxy-galaxy lensing constraints on the same lenses and sources. The tangential shear signal is then used to constrain the stellar-to-halo mass relation of central and satellite galaxies.

We model the lensing signal using an NFW profile together with the concentration-mass relation by Duffy et al. (2008), scaled by a normalisation factor that we fit for. We assume a functional form for the stellar-to-halo mass relation in the form of a single power-law and fold it through our model, thus directly fitting for the normalisation and slope of the stellar-to-halo mass relation. The lens model is used to calculate the tangential shear profile that is then fitted to the measured tangential shear profile from the GAMA and KiDS data as well as to directly predict the two cartesian components of the galaxies' ellipticities used in our two-dimensional method.

We find that the the stellar-to-halo mass relation can be successfully measured using the two-dimensional method, with a better statistical power than the traditional one-dimensional method using the stacked tangential shear measurements. Both methods give us similar results for the stellar-to-halo mass relations, showing that the two-dimensional method is indeed a robust way to measure properties of the galaxy-halo connection, without using statistically equivalent samples as in the case of the one-dimensional method, nor using more complicated halo models or relying on support from other probes. The obtained stellar-to-halo mass relations are broadly in agreement with the literature, although further study of remaining biases in our analysis is needed and the measurements will be improved shortly.

Following this pilot analysis we will refine the analysis by the inclusion of all the available overlapping KiDS and GAMA data, together with the inclusion of the remaining ungrouped galaxies will make the two-dimensional method more accurate, less biased and statistically more powerful than the one-dimensional one.

ACKNOWLEDGEMENTS

AD and KK acknowledge support from grant number 614.001.541 and HH acknowledges support from Vici grant number 639.043.512, both financed by the Netherlands Organisation for Scientific Research (NWO). KK acknowledges support by the Alexander von Humboldt Foundation.

This research is based on data products from observations made with ESO Telescopes at the La Silla Paranal Observatory under programme IDs 177.A-3016, 177.A-3017 and 177.A-3018, and on data products produced by Target/OmegaCEN, INAF-OACN, INAF-OAPD and the KiDS production team, on behalf of the KiDS consortium.

GAMA is a joint European-Australasian project based around a spectroscopic campaign using the Anglo-Australian Telescope. The GAMA input catalogue is based on data taken from the Sloan Digital Sky Survey and the UKIRT Infrared Deep Sky Survey. Complementary imaging of the GAMA regions is being obtained by a number of independent survey programs including GALEX MIS, VST KiDS, VISTA VIKING, WISE, Herschel-ATLAS, GMRT and ASKAP providing UV to radio coverage. GAMA is funded by the STFC (UK), the ARC (Australia), the AAO, and the participating institutions. The GAMA website is <http://www.gama-survey.org>.

This work has made use of Python (<http://www.python.org>), including the packages `numpy` (<http://www.numpy.org>) and `scipy` (<http://www.scipy.org>). Plots have been produced with `matplotlib` (Hunter 2007).